Phonon anomalies and phonon-spin coupling in oriented $PbFe_{0.5}Nb_{0.5}O_3$ thin films

Margarita Correa,[1] Ashok Kumar,[1] Shashank Priya,[2] R. S. Katiyar,[1,*] and J. F. Scott[3]
[1]*Department of Physics and Institute for Functional Nanomaterials, University of Puerto Rico, San Juan, Puerto Rico 00931-3343*
[2]*Center for Energy Harvesting Materials and Systems (CEHMS), Department of Materials Science and Engineering, Virginia Tech, Blacksburg, Virginia 24061, USA*
[3]*Department of Physics, Cavendish Laboratory, University of Cambridge, Cambridge CB3 OHE, United Kingdom*
(Received 9 June 2010; published 18 January 2011)

We present Raman data on both single-crystal and thin-film samples of the multiferroic $PbFe_{0.5}Nb_{0.5}O_3$ (PFN). We show first that the number and selection rules of Raman lines are compatible with a face-centered-cubic *Fm-3m* structure, as is known in other ABO_3 relaxors, such as $PbSc_{1/2}Ta_{1/2}O_3$. We then compare Raman data with anomalies in magnetization and the dielectric constant near the magnetic-phase-transition temperature (T_N), the diffuse ferroelectric-phase-transition temperature (T_m), and the pseudostructural-phase transition temperature (Burns temperature $\sim T_B$). The temperature evolution of the Raman spectra for the PFN film shows measurable changes in phonon positions, intensities, and full width at half maxima near 200, 410, and 650 K—temperatures that match well with experimentally observed T_N, T_m, and T_B, respectively. The increase in frequency with increasing temperature for the lowest-energy F_{2g} phonon mode is particularly unexpected. These changes suggest the transition of the crystal structure from an ordered phase to a disordered phase near T_B. The Raman study revealed phonon anomalies in the vicinity of T_m and T_N that are attributed to the dynamical behavior of polar nanoregions and spin-phonon coupling owing to its relaxor and multiferroic nature, respectively, which is well supported by dielectric and magnetic properties of the PFN thin film. Softening of the Fe-O mode was observed near the T_N. We correlate the anomalous shift of the Fe-O mode frequency with the normalized square of the magnetization sublattice; agreement with the experimental results suggests strong spin-phonon coupling near T_N owing to phonon modulation of the superexchange integral; however, the shifts in frequency with temperature are small (<3 cm^{-1}).

DOI: 10.1103/PhysRevB.83.014302 PACS number(s): 77.55.Nv, 77.80.Jk

I. INTRODUCTION

Lead iron niobate (PFN) is a complex perovskite material that was originally reported by Smolenkii *et al*. in late 1950's.[1] PFN belongs to the class of materials having two or more order parameters (elastic, electric, or magnetic) coexisting in the same phase. Among single-phase multiferroic materials, very few exhibit significant coupling of their magnetic and electric order, and these are quite promising for magnetoelectric (ME) applications.[2] Single-phase multiferroics belonging to the $AB'B''O_3$ complex perovskite family, such as $PbFe_{0.5}Nb_{0.5}O_3$ (PFN), $PbFe_{0.5}Ta_{0.5}O_3$ (PFT), and $PbFe_{0.67}W_{0.33}O_3$ (PFW), have gained interest because in these materials magnetic (d^5) Fe^{3+} ions and nonmagnetic (d^0) Nb^{5+}, Ta^{5+}, and W^{6+} ions have a common B site. The (d^5) ion in the BO_6 octahedral sites leads to ferromagnetic (FM) order, while the (d^0) ions in similar lattice positions help provide ferroelectric (FE) order. Thus, these materials are good candidates to study multiferroicity and possible ME coupling in a single-phase material.[1,3–5]

The dielectric, magnetic, and magnetoelectric properties of PFN have been studied in single-crystal, ceramic, and thin-film forms.[1,6–15] Bulk PFN undergoes a paraelectric (PE) to FE phase transition with a Curie temperature (T_C) between 379 and 385 K.[1,6,7] In the case of PFN films, a diffuse phase transition (DPT) with frequency dispersion has been reported.[8,9] Bulk PFN exhibits a paramagnetic (PM) to antiferromagnetic (AFM) phase transition with a Néel temperature (T_N) of 140 K.[10,11] However, ferromagnetic (FM) order has been reported sometimes at low temperature[12] ($\sim$9 K) or even room temperature.[13] Experimentally observed dielectric anomalies owing to ME coupling were reported in PFN single crystals.[14] Monte Carlo simulations of ME coupling provided reasonable agreement between the simulated and the experimental results of PFN single crystals.[15] Although PFN does not exhibit B-site cation ordering, it shows normal long-range dipole order in the FE phase[16] of single crystals and ceramics. However, PFN films have been reported as ME relaxors, that is, having a simultaneous frequency dispersion of both the electrical and magnetic susceptibilities[17]—a relaxor FE with weak FM properties.[8,9] The detailed structural, dielectric, and magnetic properties of the PFN films are reported elsewhere.[9]

Our PFN films were highly oriented with an in-plane epitaxial relationship PFN [100] ∥ LSCO [100] MgO [100]. The temperature evolution of the dielectric constant showed a diffuse FE phase transition with frequency dispersion. The dielectric maximum temperature (T_m) shifted from 337 K (5 kHz) to 380 K (100 kHz). The frequency dispersion of the dielectric constant follows a Vogel-Fulcher law and gives an activation energy of 5.1 meV (equivalent to 62 K) and a freezing temperature of 325 K. The low activation energy of PFN films (62 K) as compared to the experimental measuring temperature indicates its nonequilibrium state as in a glassy system.[18,19] Besides the frequency-dependent dielectric maxima, we observed two more features in the temperature evolution of the dielectric constant of PFN thin

films: One was in the vicinity of T_N, where a small kink ∼170 K was observed; the second was a bump at ∼600 K near the Burns temperature (T_B). We ascribed the former dielectric anomaly to strong spin-dipole coupling that has been found already in PFN single crystals and ceramics.[7,12,14] The latter anomaly was associated with structural changes in the sample when it goes through an ordered phase to a disordered phase.

In the past decade significant effort has been devoted to understanding the physics of multiferroics and the coupling mechanisms of FE and magnetic order in ME materials. The usual approach has been to study the dielectric and magnetic properties of multiferroics under applied electric and magnetic fields in a wide temperature range. However, extraordinary spin-phonon interaction has been detected in rare-earth manganites by thermal conductivity[20] and thermal expansion[21] measurements. Raman spectroscopy has been shown to be a valuable technique in the study of optical-phonon behavior in multiferroic materials. Although phonon studies play an important role in the understanding of ferroelectricity, and this is expected to be influenced by spin correlation,[22] only in recent years has the behavior of optical phonons in multiferroics and ME multiferroics materials been studied.[23–29] Our temperature-dependent Raman study of PFN film reveals phonon anomalies in the vicinity of T_m and T_N that we ascribe to the dynamical behavior of polar nanoregions (PNRs) and spin-phonon coupling owing to its relaxor and multiferroic nature, respectively.

One important issue in the physics of FEs is the understanding of the domain structure. Among the available techniques for studying FE materials, piezoforce microscopy (PFM) has emerged as a valuable tool for local nanoscale imaging, spectroscopy, and manipulation of piezoelectric and FE materials.[30] PFM is being used to study the domain structure, its temperature evolution, switching behavior, retention, loss, and electromechanical properties of several FE materials.[30–33] In this paper, we report the room-temperature domain structure and temperature-dependent phonon anomaly of the PFN film obtained by PFM and Raman spectroscopy, respectively. The temperature-dependent Raman spectra will be correlated with magnetic and dielectric properties of the PFN film. We observed phonon anomalies around the temperature of the dielectric maximum (T_m) and the temperature of the PM-AFM phase transition T_N.

II. EXPERIMENTAL DETAILS

PFN thin films were grown on a (100)-oriented magnesium oxide (MgO) substrate with lanthanum strontium cobalt oxide (LSCO) as the bottom electrode by using the pulsed laser deposition (PLD) technique. The PFN deposition parameters were as follows: deposition temperature, 600 °C; laser energy, 250 mJ; and oxygen pressure, 200 mT. In the case of the LSCO layer, these parameters were 600 °C, 300 mJ, and 300 mT, respectively. PFN single crystals of maximum size $4 \times 3 \times 3$ mm^3 were grown by spontaneous crystallization from the mixture of polycrystalline PFN and PbO-PbF_2-B_2O_3 solvent in the appropriate proportions by using a solution technique. The mixture was sealed in a platinum crucible and then placed into a corundum crucible filled with Al_2O_3. The temperature was rapidly raised to 1200 °C, kept at that temperature for 4 h, and then finally cooled to 900 °C at a rate of 2–3 °C h^{-1}. The details of the crystal structure and magnetic properties are described elsewhere.[34,35] The phase formation and crystallographic orientation of the film were analyzed by using a Siemens D500 x-ray diffractometer with Cu$K\alpha$ radiation. Dielectric properties were measured as a function of frequency (100 Hz–1 MHz) and temperature (100–650 K) by utilizing an impedance analyzer (HP4294A). A cryostat with a programmable-temperature controller (M/S MMR Technology, Inc., model K-20) was used for the temperature-dependent measurements of the above properties. The magnetic measurements were carried out by using a superconducting quantum interference device (Quantum Design MPXSXP SQUID) magnetometer. The room-temperature piezoresponse of the PFN layer was measured by a piezoforce microscope (Veeco Dimension 3100).

The Raman measurements were performed in the backscattering geometry by using a Jobin-Yvon T64000 triple spectrometer. The laser line at 514.5 nm from a coherent Argon-ion laser (Innova 90-5) was focused in a ∼2-3-μm-diameter area by using a Raman microprobe with a 80X objective. A liquid-nitrogen-cooled charge-coupled device (CCD) system collected and processed the scattering light. We collected the low-temperature spectra in vacuum from 80 to 600 K in steps of 25 K by using a LN_2 cryostat from Linkam, and the high-temperature spectra from 300 to 900 K in 50-K steps by using a high-temperature Linkam module for a Raman microprobe.

III. RESULTS AND DISCUSSION

A. Domain structure studied by PFM

Room-temperature piezoelectric phase loop, topography, amplitude, and phase images of PFN thin films are shown in Fig. 1. The PFM images of PFN film were obtained simultaneously under a small ac voltage (3 V) with no applied dc bias. In PFM measurements the amplitude and phase images yield information about the strength of the piezoelectric response and domain structure, respectively. The topography of the film revealed ellipsoid-shaped grains with an inhomogeneous size distribution [Fig. 1(a)]. The complex domain structure showed bright, dark, and intermediate contrast. The bright (dark) regions are associated with opposite polarity whereas several factors contribute to intermediate contrast.[30] The presence of intermediate contrast may be owing to randomly polarized grains, domains with the polarization vector deviating from the normal to the film plane, nonferroelectric regions, or regions with weak piezoelectric response. Bright and dark contrast in Fig. 1 suggests the existence of highly polarized areas. These areas must be self-polarized[33] because no dc bias field was applied (this often occurs upon cooling in FEs owing to strain). At room temperature the PFN film is slightly below its freezing temperature (325 K), where the growing domains freeze in (become immobile), so its domain structure reflects a frustrated FE state. The piezoelectric phase loop [Fig. 1(d)] provided evidence for the presence of the FE switching behavior.

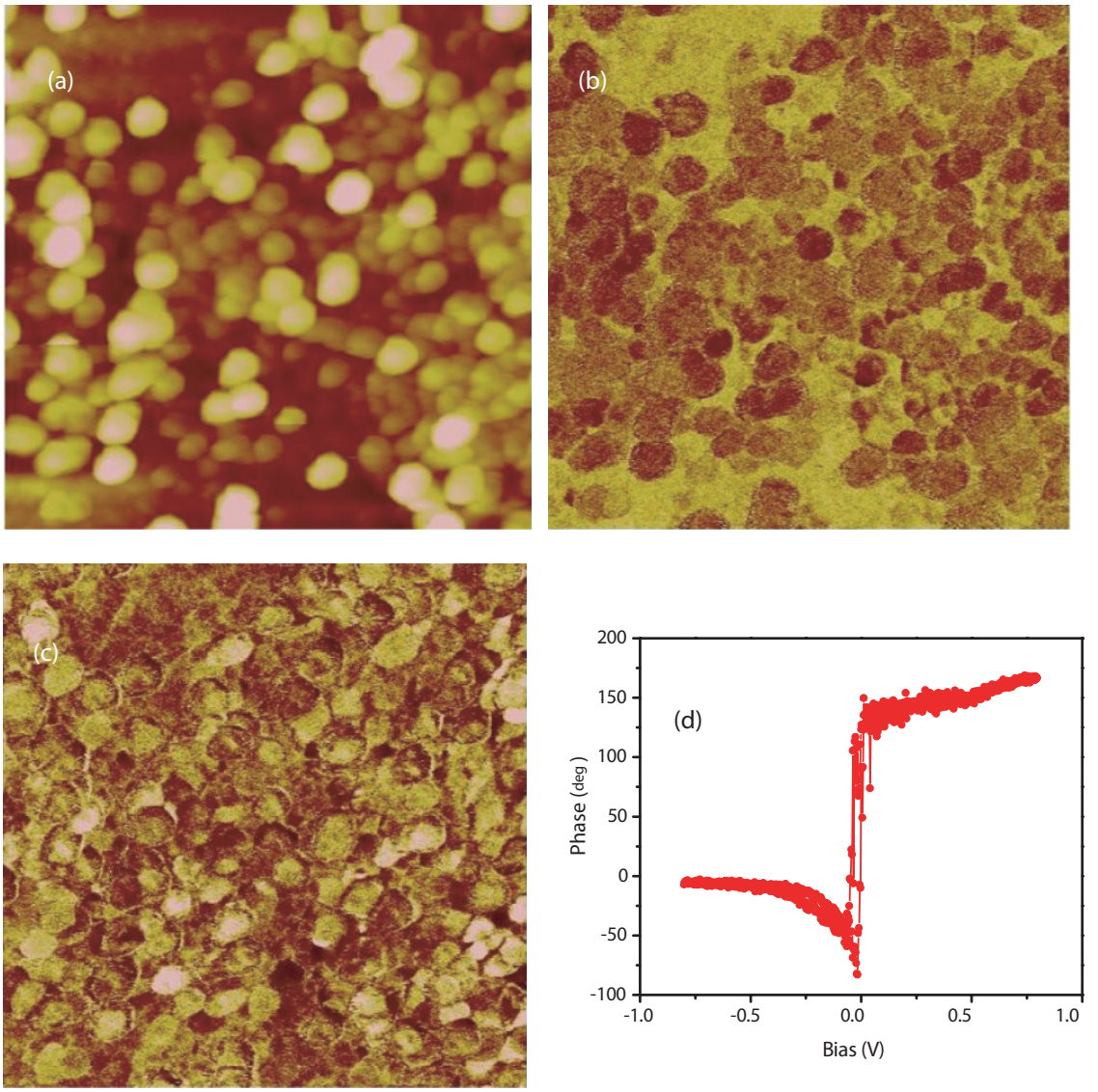

FIG. 1. (Color online) (a) Topographic (5×5 μm), (b) amplitude, (c) phase, and (d) piezoelectric phase loop of PFN thin films.

B. Temperature-dependent Raman spectra

Raman scattering data for PFN films was obtained in two distinct normal backscattering geometries, VV $[Z(XX)\bar{Z}]$ and VH $[Z(XY)\bar{Z}]$. VH denotes incident laser light polarized vertically and scattering light polarized horizontally in the laboratory frame of reference. The room-temperature spectra of both configurations of the single crystal and film are shown in Fig. 2. At this temperature the VV configuration of film and crystal consists of two relatively intense peaks at 697 and 781 cm^{-1}, a weaker peak at 427 cm^{-1}, and three broadbands at ~204, 260, and 550 cm^{-1}. The VH configuration consists of two medium-intensity bands at 206 and 261 cm^{-1}, a broadband at 522 cm^{-1}, and weak bands that may be owing to polarization "leakage" of the phonon modes from vertical polarization. At 300 K the low-frequency F_{2g} mode in the single crystal is intense and well defined but it appears as a shoulder for the film. The splitting of the A_{1g} mode discussed in the following sections is more prominent in the film than in the crystal. In this article we limit our discussion to the room-temperature Raman

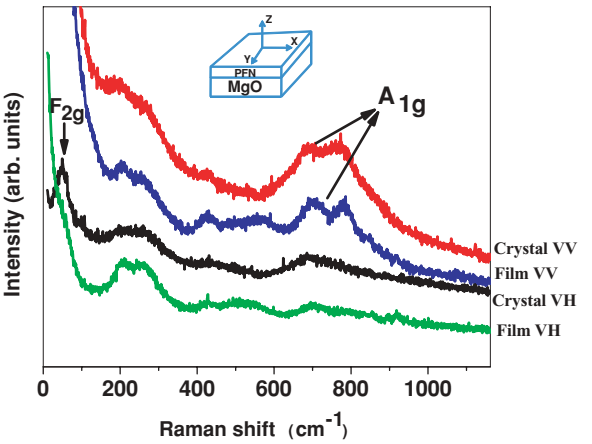

FIG. 2. (Color online) Room-temperature Raman spectra of PFN films and single crystal in VV and VH configurations.

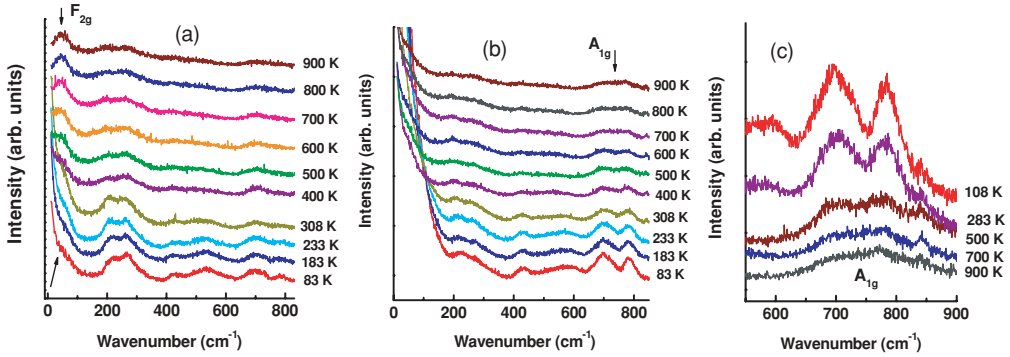

FIG. 3. (Color online) A sequence of the temperature-dependent (83–900K) Raman spectra of PFN films. (a) VH polarized (b) VV polarized, and (c) VV polarized for selected temperatures and specific frequency ranges.

study of the PFN single crystal. Detailed growth techniques, and structural and magnetic properties of the PFN single crystal were presented elsewhere.[34,35]

An ideal (primitive Pm-$3m$) cubic ABO_3 perovskite structure does not permit any Raman-active modes in its first-order vibrational spectra; because each ion is at an inversion center, all long-wavelength vibrational modes are of odd parity. However, many complex perovskites such as PFN exhibit first-order Raman spectra over a wide temperature range. $PbSc_{1/2}Ta_{1/2}O_3$ is a good example that exhibits an Fm-$3m$ face-centered-cubic structure just above its Curie temperature, dependent upon processing conditions.[36,37]

The origin of these Raman-active modes can be explained by the existence of ordered regions with a particular symmetry, disorder in the B sublattice that breaks the selection rules, or both.[38] Bulk PFN lacks B-cation ordering and behaves as a normal FE,[13] however, relaxorlike behavior has been observed in the film.[9] Figures 3(a), 3(b), and 3(c) show the temperature-dependent Raman spectra of PFN films in the VH, VV, and a closeup look of the A_{1g} mode VV configurations, respectively. The Raman spectra are consistent with the Fm-$3m$ symmetry and have $2F_{2g} + E_g + A_{1g}$ Raman-active modes and the $4F_{1u}$ infrared (IR)-active modes.[38] It is a well-known fact that the PFN crystal is a normal FE having long-range order with a tetragonal crystal structure at room temperature, whereas in the thin-film form most of the cases[9,17] show a relaxor FE with a pseudocubic structure. The assignment of phonon modes in the cubic state of the relaxor FE is still controversial and not well understood,[36–40] although it is commonly understood that lead-based relaxors are best assigned in a Fm-$3m$ cubic structure. The low-frequency F_{2g} mode arises owing to lead (Pb) localization, the high A_{1g} mode arises owing to symmetrical stretching of the BO_6 octahedral, and the modes between 180 and 320 cm^{-1} arise owing to cations off the center shift in PNRs (it is assigned for the cubic F_{1u} IR-active modes). It is worth noting that, although temperature-dependent and polarized studies allow a better understanding of the Raman modes, the collected spectra exhibit a low intensity because the set composed of an analyzer-polarizer and half-wave plate used in the setup drastically reduces the intensity. Additionally, the quartz window in the cryostat used for temperature-dependent studies reduce the laser power on the sample and indeed the scattering signal that by itself is already lower in thin films than ceramics or single crystals.

C. Phonon anomalies in the high-temperature phase

1. General observations

Figure 3(a) shows the VH-polarized Raman spectra of PFN films from 83 to 900 K. The main observed features are as follows: (i) At higher temperatures the spectra consist of one strong phonon mode with a phonon peak position (fitted) $\sim$ 64–67 cm^{-1} that corresponds to the low-frequency F_{2g} mode, plus two bands centered at $\sim$220 and 716 cm^{-1}. (ii) On decreasing temperature, the F_{2g} mode broadens and is well behaved until 600 K, but persists until 500 K. Below 500 K it becomes a shoulder, as indicated by the arrow. (iii) The phonon between 150 and 370 cm^{-1} shows changes on decreasing temperature; the peaks in this region become asymmetric at $\sim$600 K, and degenerate into two bands that change peak position, linewidth, and intensity. (iv) At lower temperatures (83 K) the spectra exhibit two bands in the frequency region between 380 and 600 cm^{-1} plus two bands more in the frequency region between 620 and 820 cm^{-1}.

2. Phonon dynamics at the regime of negative thermal expansion

The temperature dependence of the F_{2g} mode is of interest. Normally vibrational modes do not increase frequency with increasing temperature; thermal expansion causes their frequencies to decrease. The well-defined F_{2g} mode is observed at high temperature, which is almost constant (within the experimental and fitting limit) above T_B but monotonically decreases with a further decrease in temperature, similar to the deviation of the temperature dependence of the refractive index from the expected linear trend, which is typical of PEs.[37,40] In the present case, the observed dependence of phonon between 350 and 520 K can be explained on the basis of the thermal dependence change in the lattice. PFN does not exhibit thermal expansion from 350 to 520 K; instead, it undergoes thermal contraction.[41] In such a case the phonon energies should increase (as observed; see Fig 5). However, the magnitude of the increase observed, as well as the underdamping with increasing T, suggests instead that this is a kind of soft mode related to the relaxor transition. Note that a FE soft mode cannot be of even parity in the PE phase, so the exact role of this vibration in transition dynamics is unclear and merits further study.

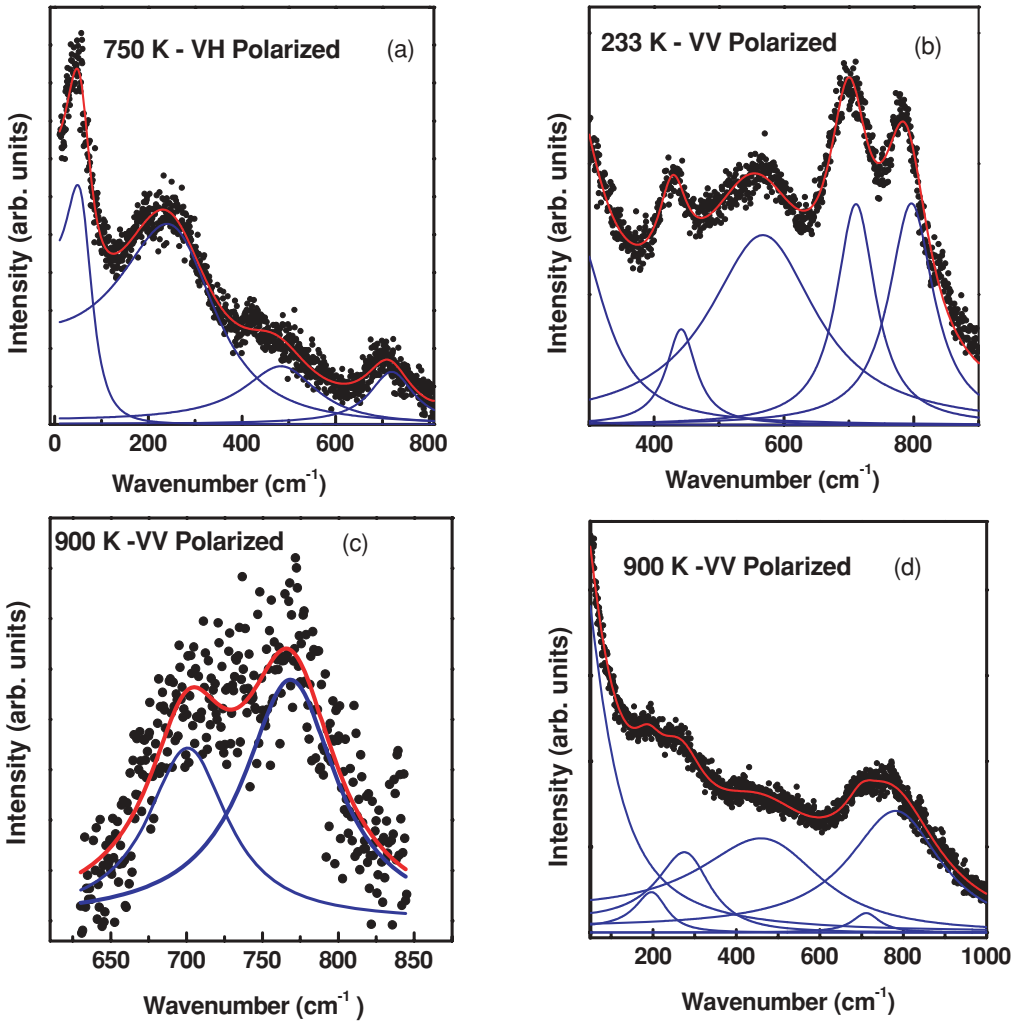

FIG. 4. (Color online) Example of the spectrum analysis at (a) 750 K and VH polarized, (b) 233 K and VV polarized, (c) and (d) 900 K and VV polarized for selected and full frequency range respectively. The points show experimental data and the solid line through points and below represents the results of fitting by the phonon modes by Eq. (1) and the constituent components of fitting (phonon modes) respectively.

3. *Phonon dynamics and the Burns temperature*

Figure 3(b) shows the temperature-dependent VV-polarized Raman spectra of PFN films. For Fm-$3m$ symmetry two Raman-active modes are expected in this configuration: the E_g and the A_{1g} mode. At higher temperatures (650 K and above), the A_{1g} mode appears to be of low intensity and has considerable thermal band broadening, but at temperatures near T_B and below it appears as a well-resolved doublet with peak frequencies at ∼780 and 700 cm^{-1}. At higher temperatures damping is strong and the intensities of both peaks in the doublet are almost similar, and then the A_{1g} mode appears as a broad asymmetric peak [see Fig. 3(c)]. This shows a strong correlation with the Burns temperature, generally considered to be near 650 K. The presence of the E_g mode in the PFN film Raman spectra is not clearly discerned. The normal vibration analysis of the complex perovskites with Fm-$3m$ symmetry shows that the A_{1g} mode represents the breathing mode of the oxygen atoms, close to that of a free oxygen octahedron.[42] Siny *et al.*[43] pointed out that the mode frequency of the A_{1g} mode changes in a series of complex perosvkite compounds as a function of the perovskite unit cell and with the changes in ionic radii. Although neither A, B', nor B'' ions move in this A_{1g} vibration, the mode still reflects subtle changes in the perovskite structure. Only the oxygen ions move, but their spacing and bonding and hence frequencies change with the size of other ions.

In order to investigate more quantitatively the temperature evolution of the observed vibrational modes in the PFN film, we analyzed the Raman spectra with the damped harmonic oscillator model (DHO).[42] Each spectrum has been fitted with the spectral response function[42,43]

$$S(v) = \sum\nolimits_i \frac{\chi_{0i}\Gamma_i v_{0i}^2 v}{\left(v^2 - v_{0i}^z + \Gamma_i^2 v^2\right)} F(v,T), \qquad (1)$$

where $F(v,T) = [n(v) + 1]$ (Stokes scattering) and $n(v) = [\exp(hv/kT) - 1]^{-1}$. The parameters in Eq. (1) [amplitude χ_0 (in arbitrary units), the mode frequency v_0, the damping constant Γ, and the temperature T] describe each phonon mode as a DHO. In the fitting routine, these parameters for all Raman bands were taken simultaneously as unconstrained variables.

At some temperatures, the Raman spectra at the lowest frequencies were fitted with a Gaussian and a Lorentzian, both centered in a zero-frequency shift that allows a better deconvolution of the spectra. Figures 4(a)–4(d) show representative graphs of the fitting routine for VV- and VH-polarized spectra at high and low temperature (the Gaussian and the Lorentzian are not shown). Owing to the high signal-to-noise ratio and considerable thermal band broadening observed at higher temperatures (above T_B) in the VV-polarized spectra, first we fit A_{1g} modes above 650 K for only the small-frequency region with two modes and later employ those parameters in the fitting of the spectra as a set of DHOs [Fig. 4(d)]. The fitted data are also presented in the Fig. 5(a) as a function of temperature, which indicates a kink near the T_B that physically represents the thermally assisted Raman shift.

Although we have analyzed most of the observed Raman bands for their energy, full width at half maxima, and integrated intensity, we will show a detailed analysis for two of the more prominent modes and also the prominent F_{1u} mode, particularly near the phase transition. The F_{2g} mode was chosen to elucidate the dynamics of the PE to diffuse FE phase transition. Because A_{1g} modes are symmetric, they play no direct role in the high-temperature phase of any symmetry-breaking phase transition. However, we found a correlation between the temperature evolution of the A_{1g} mode and the temperature regimes where mobile PNRs and static PRNs exist in the PFN film, and in the vicinity of the PM-to-AFM temperature phase transition.

Temperature-dependent A_{1g} Raman active modes are illustrated in Fig. 5(a). The temperature evolution of the observed A_{1g} vibrational modes of the PFN film is analyzed by the DHO model.[42] The A_{1g} mode represents the dynamic evolution of the relaxor FE state in PFN films. The A_{1g} modes fit with two well-defined phonon modes below the T_B, and these modes appear to be of low intensity and show considerable thermal band broadening above T_B. The observation of two phonon modes below T_B matched with the complex B-site relaxor family,[43–46] unlike classical relaxors ($PbMg_{1/3}Nb_{2/3}O_3$, $PbSc_{1/2}Ta_{1/2}O_3$), where only one singlet peak is observed.[16,18,37] The so-called two-phonon-mode behavior was introduced for $Si_{1-x}Ge_x$ systems,[45] and was later also observed for complex relaxor systems as mentioned above. The low Raman band at 698 cm^{-1} corresponds to Fe-O stretching, whereas the 788 cm^{-1} band represents Nb-O stretching. In such a system the vibration associated to the two-band mode do not couple owing to their chemical origin. The kink in the Raman shift of two bands above T_B is mainly owing to the change in the disorder-to-order state. We observe the Burn temperature and lattice stability for PFN film at 650 K, which matched the kink in the frequencies of the doublet and support the transformation of the disordered-to-ordered state.

Figure 5(b) shows the Raman shift of the F_{2g} mode in the temperature window (100–900 K), where it appears as a sharp phonon peak above 500 K, and below 500 K where it appears as a shoulder. We deconvoluted through the Gaussian-Lorentzian fit as shown in Fig. 4. The mode frequency (Raman shift) of the F_{2g} branch exhibited a downshift in frequency by ~3.0 cm^{-1}, however, it decreases in two steps from 900 to 650 K and from 650 to 350 K, and below that it remains fairly constant. Above

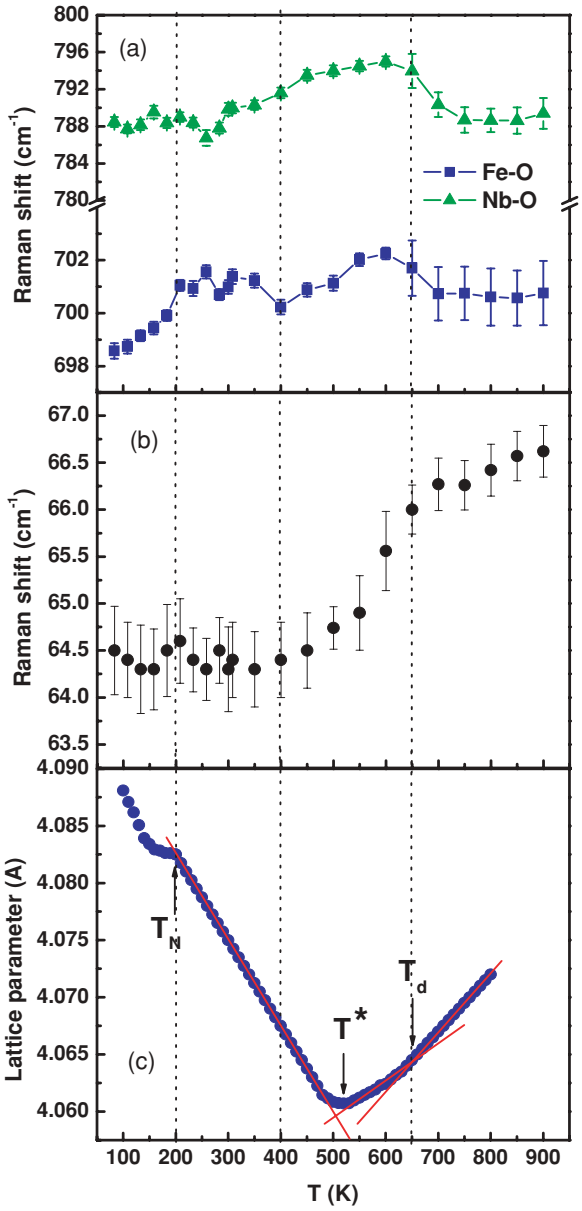

FIG. 5. (Color online) (a) Raman shift of the A_{1g} mode from 83 to 900 K. (b) Raman shift of the F_{2g} mode from 83 to 900 K. (c) Temperature evolution of the lattice parameter for a PFN film.

T_B it is practically constant, where it started to soften from T_B to T^* owing to the temperature dependence deviation of the refractive index of normal PE materials. Further softening of the F_{2g} mode up to 350 K may be owing to the lattice contraction, as can be seen in Fig. 5(c). Peng *et al.*[41] reported the temperature evolution of the lattice parameter of the PFN film grown by the PLD technique (comparable to us). Here we reproduced the lattice constant behavior of the PFN film with the reported value of Peng *et al.* [Fig. 5(c)]. The evolution of the lattice parameter clearly shows three anomalies at 650, 510, and 200 K. These anomalies were respectively ascribed to the Burns temperature T_B, at which the PNRs begin to nucleate, T^* related to the appearance of static PNRs, and T_N as the PM-to-AFM phase transition temperature. Although T_N for these films is higher than T_N for bulk (145 K), they ruled out any

strain effect on T_N but attributed the shift in T_N to a variation in the stoichiometric ratio of high-spin Fe^{3+} cation taking place during film growth. The reported lattice anomalies at T_N and T_B are consistent with our own results on the dielectric, magnetic, and Raman studies of PFN film. In addition, 500 K is the crossover temperature from a narrowed F_{2g} mode at high temperatures to an abruptly broadened shoulder, suggesting a qualitative change in coherence length for nanoregions setting in near 500 K.

Regardless of the changes described above in the F_{2g} and A_{1g} modes between 600 and 900 K, the overall spectral signature does not change notably in this temperature range. That is not the case for temperatures below 600 K, where new spectral signatures such as new Raman lines and line splittings are observed in both geometries. We inferred above the appearance of a local *Fm*-3*m* space symmetry in the PFN film. At 600 K and below, the formation of inequivalent oxygen octahedra with Fe^{+3} and Nb^{+5} cations reduces this symmetry and causes a doubling of the A_{1g} mode, as first discussed in tungstates and molybdates with two MO_4 ions per unit cell[47] and later by so-called two-phonon modes in a different system, as described above.

D. Phonons in the low-temperature phase

1. Qualitative behavior

Figure 6 shows a band softening of 216 cm^{-1} (at 100 K), which arises owing to off-center *B*-site distortion and local cation displacement. This particular mode softens ~18 cm^{-1} up to 600 K. The major Raman shift takes place near the DPTs. All of the modes between 180 and 320 cm^{-1} arise owing to the cation off-center shift in the PNRs (it is assigned for the cubic F_{1u} IR-active modes). Among these modes, the Nb-O stretching mode (216 cm^{-1}) is more sensitive to FE long-range ordering. The freezing temperature, i.e., long-range FE ordering of PFN thin films, is ~325 K; below this temperature softening is less prominent. The important questions are as follows: (i) Why does this mode show significant softening near the diffuse phase transition? (ii) What is responsible for this effect? The answers may be driven by two different mechanisms. It may be owing to (i) a lead site off-shift, a *B*-site octahedral tilt, and local cation ordering in PNRs, or (ii) cubic-phase F_{1u} infrared active mode ("silent mode"). The second reason is most unlikely.

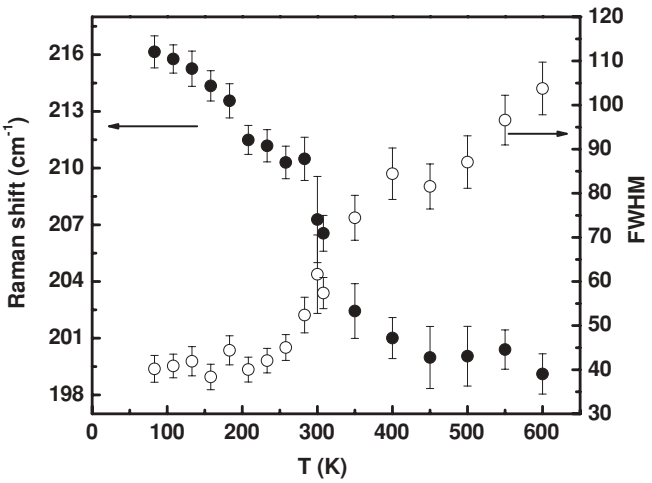

FIG. 6. Temperature evolution of the frequency, linewidth, and intensity of Nb-O band near 180–350 cm^{-1} from 83 to 600 K.

The PFN single crystal and ceramics behave as a normal FE; their *A* site is occupied by lead, and the off-shift of lead is vital for spontaneous polarization. The PFN thin film showed a relaxor FE behavior and DPT, which in turns give some fraction of spontaneous polarization. As we know, the two classical FEs, $BaTiO_3$ and $PbTiO_3$, show spontaneous polarization owing to hybridization of the 3*d* states of the *B*-positioned Ti ions and 2*p* states of off-center *B*-site oxygen distortion.[48] Lead off-shift also gives spontaneous polarization in lead-based FEs. Most likely this reason is more responsible for band softening.

On the other hand, the structural change allows also the presence in Raman spectra of the nominally F_{1u} IR-active mode ("silent mode") in which the B'/B'' ions participate, and it is affected by the mass of those ions. The F_{1u} mode is located in the frequency region from 150 to 380 cm^{-1} in ABO_3 perovskites, e.g., at 173 cm^{-1} in cubic $SrTiO_3$,[47,49] and, as can be seen in the VH-polarized Raman spectra, it splits into two bands. Because Nb ions have a larger mass compared to Fe ions, the band with the lower frequency corresponds to the vibration mode of the Nb-O bond, whereas that with higher frequency is the vibrational mode of the Fe-O bond.

2. Magnetic interactions with phonons

It is worth noting that, from 83 to 600 K the magnetic, dielectric, and FE properties of the PFN film were studied and reported elsewhere.[9] The temperature evolution of the dielectric spectra of the PFN film showed three anomalies: (1) a kink near the Néel temperature (~170 K); (2) a DPT (327–380 K) with frequency dispersion near the temperature at which the dielectric maxima occur; and (3) an almost frequency-independent maximum at 600 K, suggesting weak ME coupling, relaxor behavior, and a structural phase transition, respectively.[9] Dielectric properties and magnetic hysteresis revealed the coexistence of relaxor ferroelectricity and weak ferromagnetism at room temperature in PFN films.[8,9,17] Although neither the relaxor state nor the magnetic transitions are accompanied by a transition to a homogeneous single-phase state with long-range order, we still observe phonon anomalies in the vicinity of T_N and T_m.

The change in the frequency of the breathing-type motion of both oxygen octahedra as a function of temperature is shown in Fig. 7. The intensity and linewidth of both modes follow a similar behavior: The intensity increases with decreasing temperature and the linewidth decreases on cooling [see Fig. 3(c)]. However, the temperature evolution of the energy for both modes differs significantly, and their changes can be correlated with the magnetic and dielectric properties exhibited by the film. In the low-temperature phase (600–83 K) phonons respond to the dynamical changes in FE and magnetic order. We can identify three temperature regions where different trends are observed: region I from 600 to 400 K, region II from 400 to 200 K, and region III from 200 to 83 K. The

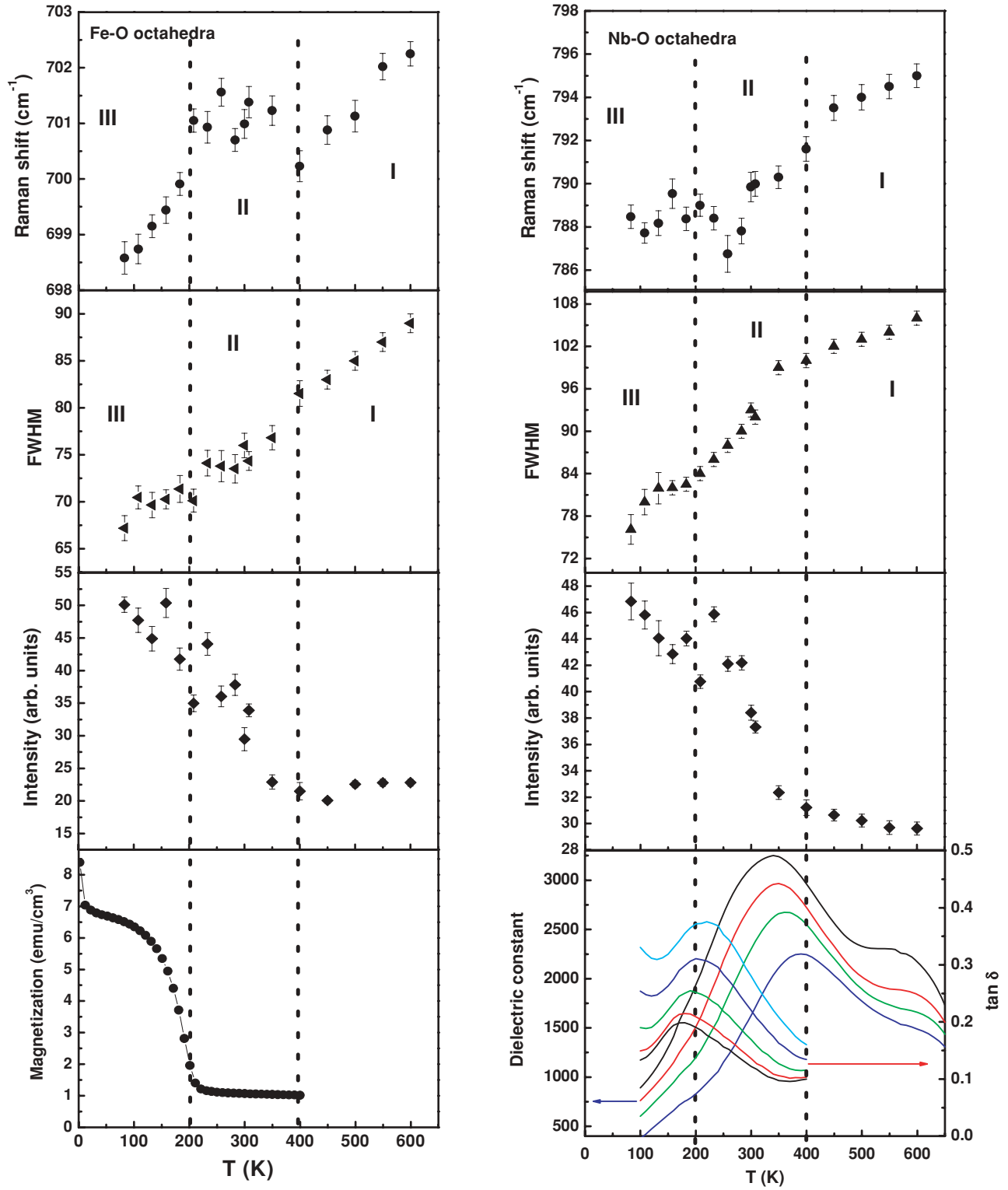

FIG. 7. (Color online) Temperature evolution of the frequency, linewidth, and intensity of Nb-O and Fe-O octahedrons from 83 to 600 K, FC (100 Oe) magnetization, and dielectric response as a function of temperature of PFN films.

overall change in the frequency of the Fe-O octahedra ($\Delta\omega$) is $\sim$3.7 cm^{-1}, but it does not change monotonically; instead it is perturbed in the full temperature range. When the material enters the temperature region with magnetic order (region III), the frequency of the Fe-O octahedra mode drops. This kind of abrupt decrease may be owing to the change in the magnetic ordering at $\sim$200 K. The magnetic ordering data are supported by the field-cooled (FC) temperature-dependent magnetization: The M-vs-T curve shows an abrupt increase of magnetization at 200 K. In addition, the PFN film showed a lattice anomaly at 200 K owing to the PM-AFM phase transition, as observed by Peng *et al.*[41]

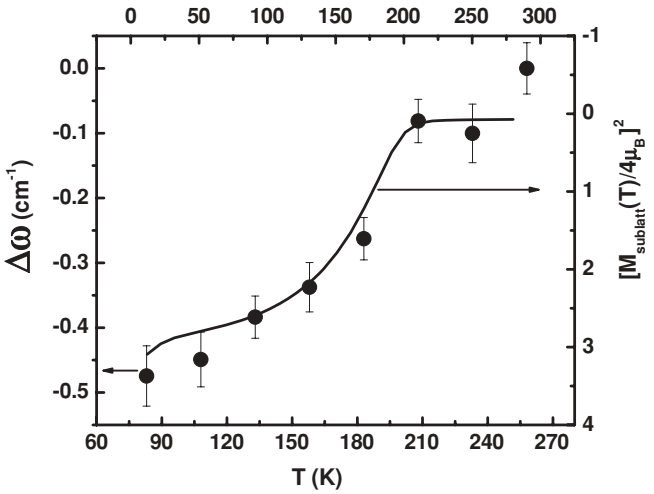

FIG. 8. Softening of Fe-O mode and change in sublattice magnetization, $\Delta\omega = (1/2\pi)[\omega(T) - \omega(258\ \mathrm{K}]$.

3. Model of Granado et al.

Magnetic ordering effects in the Raman spectra of polycrystalline $La_{1-x}Mn_{1-x}O_3$ were reported by Granado *et al.*[24] They observed a *softening* of the Mn^{3+}-O^{2-} stretching mode below T_N for orthorhombic $LaMnO_3$. This softening was associated with spin-phonon coupling owing to phonon modulation of the superexchange integral. In a nearest-neighbor approximation, they found that the frequency change with temperature of a phonon α owing to spin-phonon coupling is given by

$$(\Delta\omega)_{s\text{-ph}} \approx -\frac{2}{m\omega_\alpha}\frac{\partial^2 J_{xz}}{\partial u^2}\left(\frac{M_{\mathrm{sublatt}}(T)}{4\mu_B}\right)^2. \qquad (2)$$

The scaling of the anomalous shift of the frequency of the Mn^{3+}-O^{2-} stretching mode with the normalized square of the magnetization sublattice supports the experimental evidence that the shift is owing to spin-phonon coupling. We observed a similar scaling behavior on our experimental PFN data and also found a close correlation between the anomalous frequency drop of the Fe-O mode and magnetization at T_N. The observed softening is interpreted in terms of spin-phonon coupling owing to phonon modulation of the superexchange integral (Fig. 8).

4. Dielectric behavior and phonons

In the case of the A_{1g} mode for the Nb-O octahedra, its frequency also decreases on cooling, but the overall change in frequency ($\Delta\omega \sim 5.5\ \mathrm{cm}^{-1}$) is greater than the A_{1g} mode for the Fe-O octahedra. In Fig. 7 we can see the temperature evolution of the dielectric constant in the same temperature window of the fitted frequency of the A_{1g} mode, and we find some correlation between them. On decreasing temperature, the spatially averaged homogenous PE state changes into an inhomogeneous phase; the frequency shifts downward smoothly, and the dielectric constant shows a bump (region I). However at the boundary between regions I and II, the frequency has a sudden drop from 793.5 cm^{-1} at 450 K to 791.5 cm^{-1} at 400 K with a further decrease in the neighborhood of the diffuse phase transition temperature. In this region the dielectric constant exhibits a relaxor behavior, and the fitting of the frequency dispersion of T_m with the Vogel-Fulcher law gives a freezing temperature of 325 K. At this point, with the PNRs frozen in, the material could be in a mixed ferroglass state, as suggested by the domain structure shown by PFM; on further cooling, the frequency of the A_{1g} mode for the Nb-O octahedra just goes up and down, whereas the frequency of the A_{1g} mode for the Fe-O octahedra shows the changes discussed above owing to the onset of magnetic ordering.

IV. CONCLUSIONS

We studied the temperature evolution of the Raman spectra of a PFN film in a wide temperature range (83–900 K). The approximate local symmetry is *Fm*-3*m*. The high-temperature Raman spectra showed changes in phonon positions, intensities, linewidths, and especially the kink in the Raman shift of the A_{1g} doublet at ~650 K, suggesting an order-disorder behavior near the accepted Burns temperature and lattice constant anomalies. Our study revealed phonon anomalies in the vicinity of T_m and T_N that we ascribe to the dynamical behavior of PNRs and spin-phonon coupling owing to the relaxor FE and ME nature, respectively. We established a close correlation between the microstructural features and the dielectric and magnetic properties of the PFN film. Lattice anomalies reported for the PFN film are consistent with our results on the dielectric, magnetic, and Raman studies of PFN films. Softening of Fe-O mode, a change in magnetization sublattice, and their coupling were observed in the vicinity of the T_N scale.

ACKNOWLEDGMENTS

The authors thank Jian Jun for his help with the PFM measurement, and the Center for Intelligent Material System and Structure (CIMSS) at Virginia Tech. This work was partially supported by DoD Grants No. W911NF-06-1-0183 and DoE Grants No. DE-FG 02-08ER46526.

*rkatiyar@uprrp.edu

[1] G. A. Smolenskii, A. Agranovskaya, S. N. Popov, and V. A. Isupov, Sov. Phys. Tech. Phys. **28**, 2152 (1958).
[2] N. A. Hill, J. Phys. Chem. B **104**, 6694 (2000).
[3] A. Filippetti and N. A. Hill, Phys. Rev. B **65**, 195120 (2002).
[4] A. Falqui, N. Lampis, A. Geddo-Lehmann, and G. Pinna, J. Phys. Chem. B **109**, 22967 (2005).
[5] A. Kumar, I. Rivera, R. S. Katiyar, and J. F. Scott, Appl. Phys. Lett. **92**, 132913 (2008).
[6] M. H. Lente, J. D. S. Guerra, G. K. S. de Souza, B. M. Fraygola, C. F. V. Raigoza, D. Garcia, and J. A. Eiras, Phys. Rev. B **78**, 054109 (2008).
[7] X. S. Gao, X. Y. Chen, J. Yin, J. Wu, and Z. G. Liu, J. Mater. Sci. **35**, 5421 (2000).

[8]Li Yan, Jiefang Li, Carlos Suchicital, and D. Viehland, Appl. Phys. Lett. **89**, 132913 (2006).
[9]M. Correa, A. Kumar, R. S. Katiyar, and C. Rinaldi, Appl. Phys. Lett. **93**, 192907 (2008).
[10]V. A. Vokov *et al.*, Sov. Phys. JETP **15**, 447 (1962).
[11]G. Alvarez, R. Font, J. Portelles, R. Zamorano, and R. Valenzuela, J. Phys. Chem. Solids **68**, 1436 (2007).
[12]T. Watanabe and K. Kohn, Phase Transitions **15**, 57 (1989).
[13]S. B. Majumder, S. Bhattacharya, R. S. Katiyar, A. Manivannan, P. Dutta, and M. S. Sheehra, J. Appl. Phys. **99**, 024108 (2006).
[14]Y. Yang, J.-M. Liu, H. B. Huang, W. Q. Zou, P. Bao, and Z. G. Liu, Phys. Rev. B **70**, 132101 (2004).
[15]J.-M. Liu, Q. C. Li, X. S. Gao, Y. Yang, X. H. Zhou, X. Y. Chen, and Z. G. Liu, Phys. Rev. B **66**, 054416 (2002).
[16]C. A. Randall, A. S. Bhalla, T. R. Shrout, and L. E. Cross, J. Mater. Res. **5**, 829 (1990).
[17]A. Levstik, V. Bobnar, C. Filipič, J. Holc, M. Kosec, R. Blinc, Z. Trontelj, and Z. Jagličić, Appl. Phys. Lett. **91**, 012905 (2007).
[18]Margarita Correa, Ashok Kumar, R. S. Katiyar, and J. F. Scott, J. Phys. Condens. Matter **20**, 125211 (2008).
[19]P. B. Littlewood and R. Rammal, Phys. Rev. B **38**, 2675 (1988).
[20]P. A. Sharma, J. S. Ahn, N. Hur, S. Park, Sung Baek Kim, Seongsu Lee, J.-G. Park, S. Guha, and S-W. Cheong, Phys. Rev. Lett. **93**, 177202 (2004).
[21]C. dela Cruz, F. Yen, B. Lorenz, Y. Q. Wang, Y. Y. Sun, M. M. Gospodinov, and C. W. Chu, Phys. Rev. B **71**, 060407 (2005).
[22]A. B. Souchkov, J. R. Simpson, M. Quijada, H. Ishibashi, N. Hur, J. S. Ahn, S. W. Cheong, A. J. Millis, and H. D. Drew, Phys. Rev. Lett. **91**, 027203 (2003).
[23]R. Haumont, J. Kreisel, P. Bouvier, and F. Hippert, Phys. Rev. B **73**, 132101 (2006).
[24]E. Granado, A. García, J. A. Sanjurjo, C. Rettori, I. Torriani, F. Prado, R. D., Sánchez, A. Caneiro, and S. B. Oseroff, Phys. Rev. B **60**, 11879 (1999) .
[25]R. Palai, J. F. Scott, and R. S. Katiyar, Phys. Rev. B **81**, 024115 (2010).
[26]A. Kumar, N. M. Murari, and R. S. Katiyar, Appl. Phys. Lett. **92**, 152907 (2008).
[27]M. K. Singh, W. Prellier, H. M. Jang, and R. S. Katiyar, Solid State Commun. **149**, 1971 (2009).
[28]M. K. Singh, R. S. Katiyar, and J. F. Scott, J. Phys. Condens. Matter **20**, 252203 (2008).
[29]M. K. Singh, W. Prellier, H. M. Jang, and R. S. Katiyar, Mater. Res. Soc. Symp. Proc. **1034**, 1034 (2008).
[30]A. Gruverman, O. Auciello, and H. Tokumoto, Annu. Rev. Mater. Sci. **28**, 101 (1998).
[31]V. V. Shvartsman, A. L. Kholkin, M. Tyunina, and J. Levoska, Appl. Phys. Lett. **86**, 222907 (2005).
[32]L. Yan, X. Zhao, J. Li, and D. Viehland, Appl. Phys. Lett. **94**, 192903 (2009).
[33]A. L. Kholkin, V. V. Shvartsman, M. Woitas, and A. Safari, Mater. Res. Soc. Symp. Proc. **748**, 748 (2003).
[34]Ashok Kumar, R. S. Katiyar, Carlos Rinaldi, Sergey G. Lushnikov, and Tatjana A. Shaplygina, Appl. Phys. Lett. **93**, 232902 (2008).
[35]G. M. Rotaru, B. Roessli, A. Amato, S. N. Gvasaliya, C. Mudry, S. G. Lushnikov, and T. A. Shaplygina, Phys. Rev. B **79**, 184430 (2009).
[36]M. Dawber, S. Rios, J. F. Scott, Q. Zhang, and R. W. Whatmore, AIP Conf. Proc. **582**, 1 (2001).
[37]B. Mihailova, B. Maier, C. Paulmann, T. Malcherek, J. Ihringer, M. Gospodinov, R. Stosch, B. Güttler, and U. Bismayer, Phys. Rev. B **77**, 174106 (2008).
[38]I. G. Siny, R. S. Katiyar, and A. S. Bhalla, J. Raman Spectrosc. **29**, 385 (1998).
[39]J. Kreisel, B. Dkhil, P. Bouvier, and J.-M. Kiat, Phys. Rev. B **65**, 172101 (2002).
[40]G. Burns and B. A. Scott, Solid State Commun. **13**, 423 (1973).
[41]W. Peng, N. Lemée, M. Karkut, B. Dkhil, V. Shvartsman, P. Borisov, W. Kleemann, J. Holc, M. Kosec, and R. Blinc, Appl. Phys. Lett. **94**, 012509 (2009).
[42]R. S. Katiyar, J. F. Ryan, and J. F. Scott, Phys. Rev. B **4**, 2635 (1971).
[43]I. G. Siny, S. G. Lushnikov, R. S. Katiyar, and E. A. Rogacheva, Phys. Rev. B **56**, 7962 (1997).
[44]B. Chaabane, J. Kreisel, P. Bouvier, G. Lucazeau, and B. Dkhil, Phys. Rev. B **70**, 134114 (2004).
[45]A. S. Barker and A. J. Sievers, Rev. Mod. Phys. **47**, 1 (1975).
[46]Ashok Kumar, N. M. Murari, J. F. Scott, and R. S. Katiyar, Appl. Phys. Lett. **90**, 262907 (2007).
[47]J. F. Scott, J. Chem. Phys. **49**, 98 (1968).
[48]R. E. Cohen, Nature (London) **358**, 136 (1992).
[49]P. A. Fleury and J. M. Worlock, Phys. Rev. **174**, 613 (1968).